ORIGINAL RESEARCH ARTICLE

Effect of TiO_2 Addition on the Viscosity of Ladle Refining Slags

XIAOMENG ZHANG, ZHIYIN DENG, ZIWEN YAN, CHUNXIN WEI, and MIAOYONG ZHU

In order to understand the effect of TiO_2 on the viscosity of ladle refining slags, the viscosity of $CaO-SiO_2$-30pct Al_2O_3-5pct $MgO-TiO_2$ refining slag system was measured in laboratory, and the activation energy of the viscous flow was calculated. FTIR and Raman were also used to analyze the change of slag structures. The results show that with the increase of TiO_2 content (0 to 10 pct) in the slag system, the viscosity of the slags decreases first and then increases. A low TiO_2 content (*e.g.*, 2 pct) in the ladle slags can weaken the strength of the slag structure due to the formation of $[TiO_4]^{4-}$; while sufficient TiO_2 (*e.g.*, 10 pct) will lead to the formation of $[Ti_2O_6]^{4-}$, and further increase the degree of polymerization (DOP) of the slags. Although silicate structure can be depolymerized by TiO_2, the $[AlO_4]^{5-}$-tetrahedron structure variation plays more profound role in the change of viscosity. With the increase of the basicity ($w(CaO)/w(SiO_2)$ = 2 to 10) of the TiO_2-containing slags, the viscosity decreases. The free oxygen provided by CaO decreases the DOP of both aluminate and silicate structures. The proper addition of TiO_2 into ladle refining slags is very possible for the refining of Ti-bearing steel grades due to the positive effect on the melting point and viscosity of the slags.

https://doi.org/10.1007/s11663-024-03055-9

I. INTRODUCTION

WITH the rapid development of automotive and steel industries, more and more attention is being paid to the development of high-strength steels with excellent performance.[1–3] Generally, the element of titanium (Ti) can improve the strength, formability and weldability of steels, so Ti is widely added in automobile steel grades. In industrial production, Ti-bearing steel is often refined by $CaO-SiO_2-Al_2O_3-MgO$ slag system. After Ti alloying, due to the steel-slag equilibrium, some Ti element in the steel will transfer to the slag,[4,5] thus forming a $CaO-SiO_2-Al_2O_3-MgO-TiO_x$ system final slag. The formation of TiO_x in the slag leads to a lower yield of Ti alloy. Therefore, if a certain amount of TiO_2 was added into the refining slag system, the yield of Ti alloy can be improved.

In the refining process, lower viscosity of slags generally leads to faster mass transfer, so slag viscosity is an important factor affecting steel cleanliness. Many studies were conducted to understand the effect of slag composition on the viscosity of the slag.[6–10] Many researchers[10–31] studied the effect of TiO_2 on slag viscosity, and most of them focused on blast furnace (BF) slags, which have a silicate structure with low basicity [$R = w(CaO)/w(SiO_2)$] and a low Al_2O_3 content. In these studies,[10–31] although the contents of TiO_2 were different (0 to 45 pct) in TiO_2-containing BF slags, the viscosity of the slags generally decreased with TiO_2 content. There are different proposed mechanisms to explain the viscosity decrease of BF slags. For example, Pang *et al.*[19] proposed that TiO_2 dissociated O^{2-} to break Si-O network structure, so the viscosity of $CaO-SiO_2$-12pct Al_2O_3-8pct $MgO-TiO_2$ slag system decreased with the addition of TiO_2 from 0 to 6 pct. Liao *et al.*[23] believed that TiO_2 acted as a basic oxide in $CaO-SiO_2$-7pct MgO-12pct $Al_2O_3-TiO_2$ slags (R = 0.5 to 0.9 and $w(TiO_2)$ = 15 to 30 pct), leading to the decrease of viscosity. Zheng *et al.*[24] claimed that with the addition of TiO_2 into $CaO-SiO_2-TiO_2$ system slags (R = 1.15 to 1.21, $w(TiO_2)$ = 0 to 30 pct), the introduction of Ti^{4+} into silicate network weakened the strength of the structure thus lowered viscosity, although it enhanced the degree of polymerization (DOP). In the

XIAOMENG ZHANG is with the Key Laboratory for Ecological Metallurgy of Multimetallic Mineral (Ministry of Education), Northeastern University, Shenyang 110819, P.R. China, and with the School of Metallurgy, Northeastern University, Shenyang 110819, P.R. China, and also with the TBEA Shenyang Transformer Group Co., Ltd., Shenyang 110141, P.R. China. ZHIYIN DENG, ZIWEN YAN and MIAOYONG ZHU are with the Key Laboratory for Ecological Metallurgy of Multimetallic Mineral (Ministry of Education), Northeastern University and also with the School of Metallurgy, Northeastern University. Contact e-mail: dengzy@smm.neu.edu.cn CHUNXIN WEI is with the School of Metallurgy, Northeastern University and also with the Cold Rolling Mill, Bengang Steel Plates Co., Ltd., Benxi City 117000, Liaoning, P.R. China.

Manuscript submitted June 30, 2023; accepted February 21, 2024.
Article published online March 8, 2024.

study of Zhang *et al.*,[25] TiO_2 was considered to have a higher appealing ability to O^{2-}, resulting in a structure similar to MgO rather than CaO in the CaO-SiO_2-8pct MgO-14pct Al_2O_3-TiO_2 slag system (R = 1.0 to 1.2, $w(TiO_2)$ = 0 to 30 pct). Besides, due to the depolymerization of the structure,[24,25] the viscosity of BF slags was reported to decrease with the rise of slag basicity in these studies as well. In addition, the effects of TiO_2 on other properties (*e.g.*, surface tension,[32] foaming phenomenon,[33] density and thermal stability[34]) of BF slags were also investigated by researchers.

It is noted that ladle refining slags generally have higher Al_2O_3 contents with higher basicity in contrast to BF slags. Additionally, the content of TiO_2 in refining slags can hardly reach that of BF slags (up to 45 pct as mentioned above). As reported,[35] TiO_2 acts as an amphoteric oxide, and it may behave like an acid or basic oxide in the slags depending on the composition of the slags. Although many publications reported the effect of TiO_2 on the viscosity of BF slags as mentioned above, the effect of TiO_2 on the ladle refining slags may still be different due to the evident difference in compositions.

On the other hand, the viscosity of ladle refining slags was also widely investigated. Kim *et al.*[36] found the viscosity of low-silica calcium aluminosilicate melts decreased with slag basicity and the ratio of $w(CaO)/w(Al_2O_3)$. Zhang *et al.*[37] investigated the influence of Al_2O_3 on the viscosity of CaO-SiO_2-Al_2O_3-8pct MgO-8pct CaF_2 slag (R = 6), and the slag viscosity dramatically decreased with the increase of Al_2O_3 content. They believed that Al_2O_3 inhibited the precipitation of CaO phase in the slag. Jönsson *et al.*[38] measured the viscosity of CaO-SiO_2-Al_2O_3-MgO ladle refining slags, and the decrease of viscosity was also observed with an increasing Al_2O_3 content at 1750 K (1477 °C) to 2000 K (1727 °C). In these studies, the effect of TiO_2 was rarely involved. Although the present authors investigated the melting behaviors of TiO_2-containing refining slags in a previous study,[39] there are still few studies focusing on TiO_2-containing refining slags. Therefore, it is necessary to study the influential mechanism of TiO_2 on the viscosity of ladle refining slags.

In this study, the viscosity of a TiO_2-containing ladle refining slag system (CaO-SiO_2-30pct Al_2O_3-5pct MgO-x pct TiO_2, x = 0 to 10) was measured by a viscometer at different temperatures [1623 K to 1873 K (1350 °C to 1550 °C)], and the structure of the slag system was characterized by a Fourier transform infrared spectrometer (FTIR) and a Raman spectrometer. In addition, the activation energy of the slag system was calculated. Based on the results, the effect of TiO_2 on the viscosity of the ladle refining slag system was discussed.

II. EXPERIMENTS

A. *Viscosity Measurement*

The chemical reagents of CaO, SiO_2, MgO, Al_2O_3, and TiO_2 were used to make the synthetic slags. Similar preparation method of synthetic slags was also considered in previous studies.[39] Table I shows the weighed composition of each slag. The content of TiO_2 in the slags ranged from 0 to 10 pct, and the basicity [R = $w(CaO)/w(SiO_2)$] of the slags varied from 2 to 10.

Table I. Compositions of Experimental Slags (Weight Pct)

Slag No.	CaO	SiO_2	Al_2O_3	MgO	TiO_2	Basicity R
A1	55.71	9.29	30.00	5.00	—	6
A2	54.00	9.00	30.00	5.00	2.00	6
A3	51.43	8.57	30.00	5.00	5.00	6
A4	49.71	8.29	30.00	5.00	7.00	6
A5	47.14	7.86	30.00	5.00	10.00	6
B1	40.00	20.00	30.00	5.00	5.00	2
B2	53.33	6.67	30.00	5.00	5.00	8
B3	54.55	5.45	30.00	5.00	5.00	10

The viscosity of the slags was measured by the rotating cylinder method using RTW-10 viscometer (Northeastern University, China). Figure 1(a) illustrates the sketch of RTW-10 viscometer, which is consisted of an electric resistance furnace and a viscometer. As shown, a B-type thermocouple was seated below the crucible to measure the temperature of the slag. Since the viscosity of castor oil at a specific temperature is known, the viscometer with a Mo spindle (see Figure 1(b)) was calibrated by castor oil before measurement. 140 g mixed slag was put in a graphite crucible (OD50 mm, ID40 mm, H 200 mm), and then placed in the hot zone (D 50 mm, L 250 mm) of the PID-controlled furnace (accuracy: ±1 K). To maintain the atmosphere, high purity (>99.999 vol pct) argon gas was injected into an Al_2O_3 reaction tube at a flow rate of 1 NL/min. After the furnace was heated up to 1773 K (1500 °C), the Mo spindle was hung above the liquid level to heat it to the same temperature. Once the slag was entirely melted, the Mo spindle was then slowly dipped into the liquid slag and rotated at 200 rpm. The distance between the tip of the Mo spindle and the bottom of the crucible was 10 mm. During measurement, the temperature dropped gradually at a rate of 3 K/min, until the slag viscosity roughly reached 4 Pa·s. After the measurement, the furnace was reheated to 1773 K (1500 °C) to take the spindle out from the slag. The crucible with the slag was eventually quenched with water (no direct contact with slag).

B. *FTIR and Raman Spectroscopy Analysis*

1. *Pre-melted slag preparation*

After viscosity measurement, the quenching of the slags was insufficient. So completely glassy slags were difficult to be obtained for FTIR and Raman spectroscopy analysis. To solve this problem, another vertical electric resistance furnace was employed to prepare pre-melted slags. Figure 2 gives the schematic diagram of the furnace. As shown, besides an Al_2O_3 reaction tube, a water-cooled quenching chamber is also equipped in the furnace. Both the reaction tube and quenching chamber were sealed by O-rings, and they can be vacuumized by a vacuum pump. Before

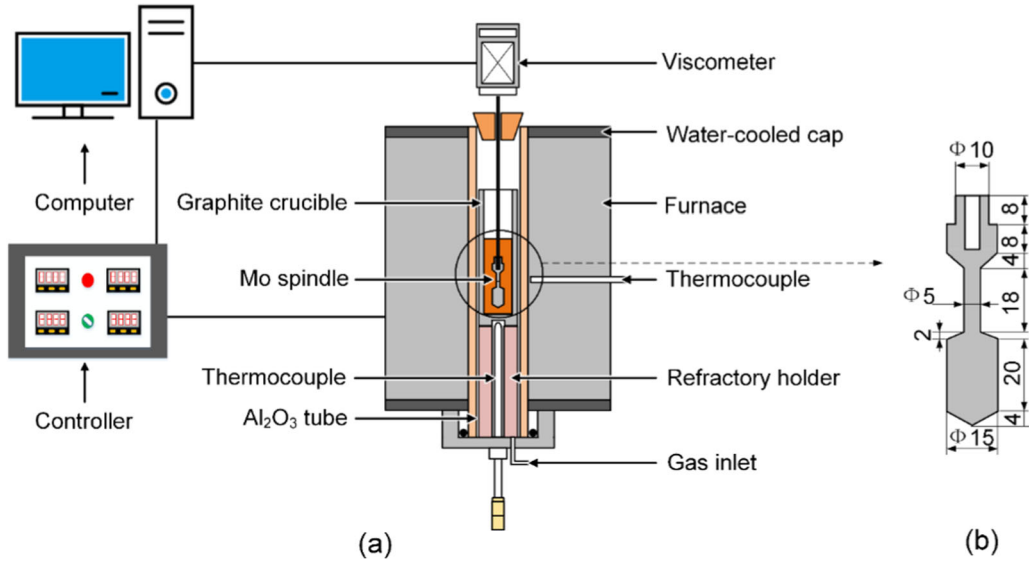

Fig. 1—Experimental setup for viscosity measurement. (*a*) Viscometer system; (*b*) Dimensions of Mo spindle.

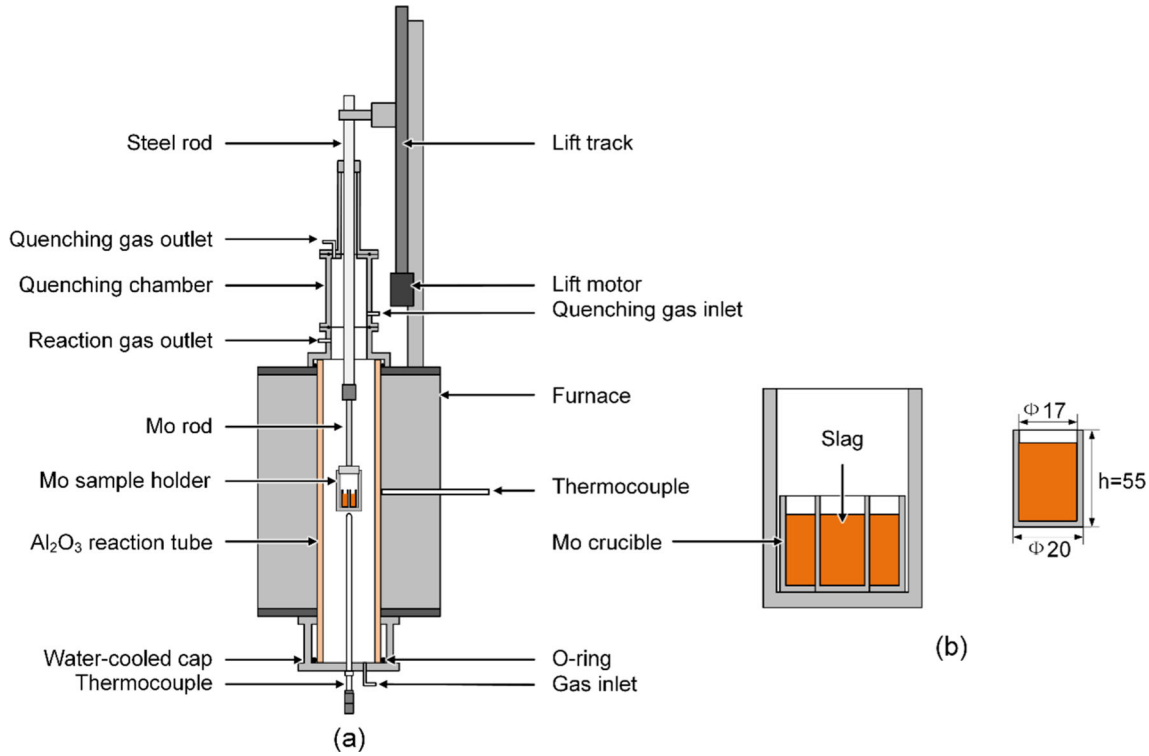

Fig. 2—Experimental setup for quenched slags. (*a*) Furnace; (*b*) Sample holder with crucibles.

experiments, the well-mixed chemical reagents were put in a Mo crucible, and further placed in a Mo sample holder. Then, the sample holder was driven by a motor to move to the hot zone of the furnace. After that, the furnace was sealed and evacuated, and high purity (>99.999 vol pct) argon gas was introduced into the furnace at a flow rate of 0.2 NL/min. When the furnace was heated up to 1773 K (1500 °C), the slag was melted for 2 h. Thereafter, the sample holder was quickly lifted to the quenching chamber. Meanwhile, a high flow rate of argon gas was injected into the chamber to strengthen quenching. Thus, glassy slag was obtained.

2. *Analysis*

The pre-melted slags were ground into fine powders. The quenched phases in the pre-melted slags were determined by X-ray diffraction (XRD, Ultima IV, Rigaku). In order to understand the relationship

between the viscosity and the structure of the slags, FTIR and Raman spectroscopy analyses were carried out. 2.0 mg of the slag powders and 300 mg of KBr were well-mixed and pressed into a thin film for FTIR analysis (Nicolet iS10, Thermo Fisher Scientific). The glass samples were also analyzed by a micro-Raman spectrometer (inVia Qontor, Renishaw) at room temperature with excitation wavelength of 532 nm and a 1-mW semiconductor laser as the light source. According to previous studies,[40] the wavenumber of ladle slags was generally within the range of 400 to 1200 cm^{-1}. Therefore, the wavenumber for FTIR and Raman spectra was chosen in this range. The detailed assignments of the FTIR and Raman spectra are introduced in the following sections.

III. RESULTS

A. *Effect of TiO_2 on Viscosity*

Figure 3 plots the viscosities of the slags ($R = 6$) with different TiO_2 contents at different temperatures. As shown in Figure 3, when 2 pct of TiO_2 is added into the slags, the lowest viscosity is obtained at high temperatures [>1723 K (1450 °C)]. With further addition of TiO_2 in the slags, the viscosities of the slags increase. It is noted that the viscosities of some slags increase sharply at a certain temperature. This temperature is considered as breaking point temperature (T_{Br}).[41] When no TiO_2 is added, the highest T_{Br} [1703 K (1430 °C)] is obtained; T_{Br} has the lowest value of 1643 K (1370 °C) when the content of TiO_2 is 5 pct. When TiO_2 further increases to 10 pct in the slags, there is no obvious T_{Br} as a result. This is probably due to some phases formed at a certain temperature. As reported in literature,[41] T_{Br} is close to the liquidus temperature of slag. The present authors also measured the melting points of these slags in a previous publication,[39] and found that the melting points decrease first and then decrease with the addition of TiO_2 in the slags. The T_{Br} shown in Figure 3 is in line with the previous publication.

B. *Effect of Basicity on Viscosity*

The effect of basicity on the viscosity of CaO-SiO_2-30pct Al_2O_3-5pct MgO-5pct TiO_2 slags at various temperatures is shown in Figure 4. The results show that with the climb of slag basicity from 2 to 10, the viscosity decreases at high temperatures, and T_{Br} presents a declining trend first and then increases. When the basicity is 8, T_{Br} obtains the lowest value [1613 K (1340 °C)]; T_{Br} reaches the highest value of 1773 K (1500 °C) when $R = 2$.

C. *FTIR Spectra of Slag*

The XRD patterns of the quenched slags are shown in Figure 5. It is seen from Figure 5 that the quenched slags are fully amorphous. Therefore, FTIR and Raman analyses are reasonable. Figure 6 shows the FTIR

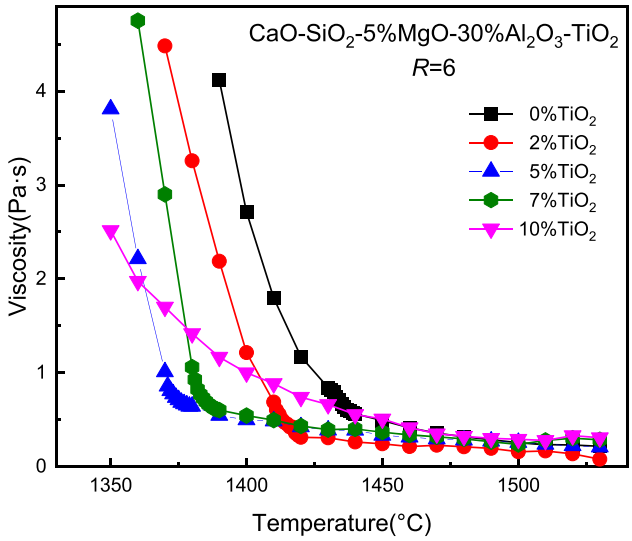

Fig. 3—Effect of TiO_2 content on slag viscosity.

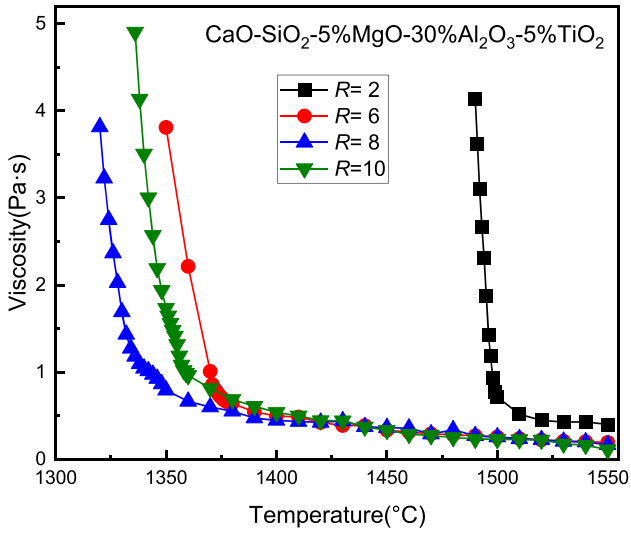

Fig. 4—Effect of basicity on slag viscosity.

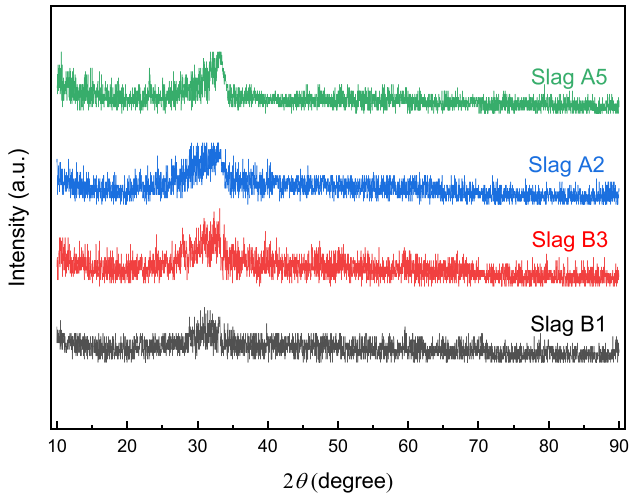

Fig. 5—XRD patterns of quenched slags.

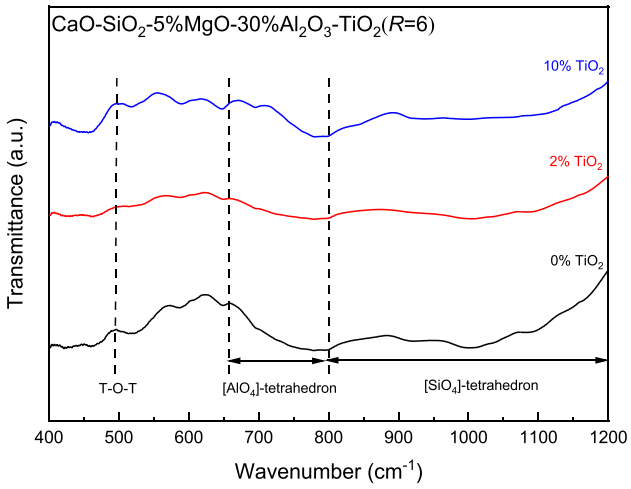

Fig. 6—FTIR spectra of slags with different TiO_2 contents (R = 6).

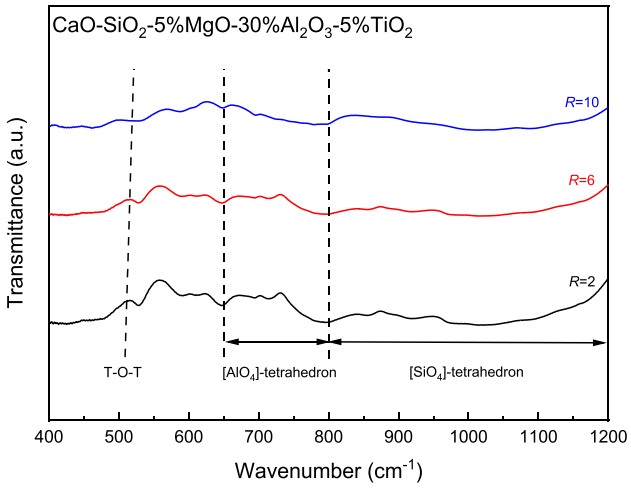

Fig. 7—FTIR spectra of slags with different basicity ($w(TiO_2)$ = 5 pct).

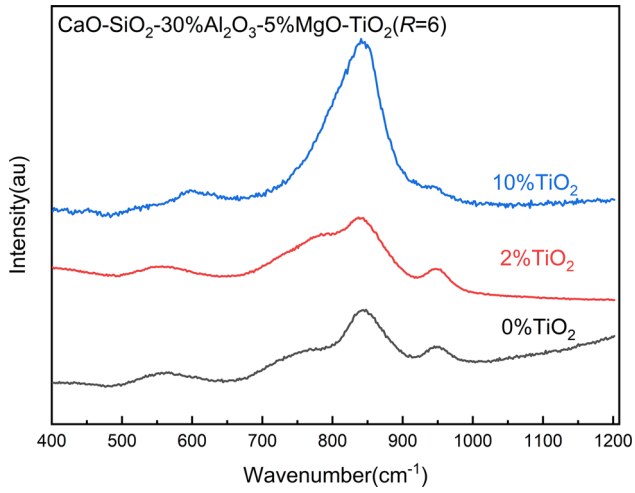

Fig. 8—Effect of TiO_2 content on Raman spectra.

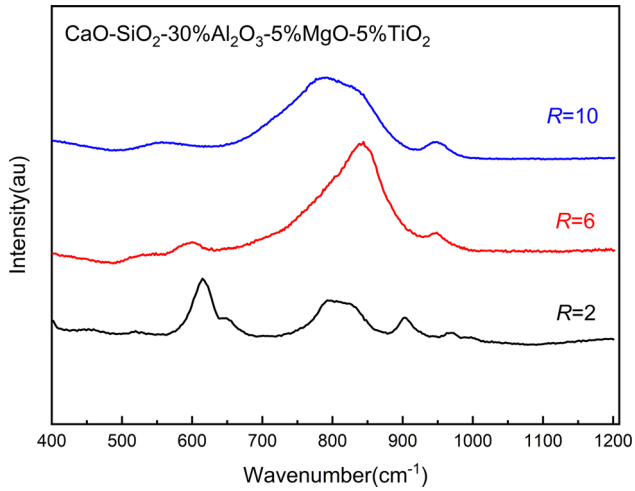

Fig. 9—Effect of basicity on Raman spectra.

spectra of the as-quenched slags with different TiO_2 contents. Based on previous studies,[38–41] the symmetric stretching vibration of the $[SiO_4]^{4-}$-tetrahedron (800 to 1200 cm^{-1}), the stretching vibration of the $[AlO_4]^{5-}$-tetrahedron (660 to 800 cm^{-1}), and T-O-T (T: Si or Al) band vibration (~500 cm^{-1}) are mainly considered in the FTIR spectra. As shown in Figure 6, with the increase of TiO_2 content from 0 to 10 pct, the peaks of the T-O-T band vibration decrease first and then increase. When the TiO_2 content is 2 pct, the $[AlO_4]^{5-}$-tetrahedron becomes less pronounced. It gets deeper when the content of TiO_2 is 10 pct in the slag. In addition, $[SiO_4]^{4-}$-tetrahedron also becomes less pronounced with TiO_2 addition.

The influence of slag basicity on the FTIR spectra is shown in Figure 7. As can be seen, when the basicity of the slags increases from 2 to 10, the T-O-T band vibrations become weaker and weaker, and the depth of $[AlO_4]^{4-}$-tetrahedron vibration band decreases as well. It means the complex aluminate structure is depolymerized. In addition, the $[SiO_4]^{4-}$-tetrahedron becomes less pronounced, indicating that the silicate structure in the slag plays limited role due to the low SiO_2 content.

D. *Raman Spectra of Slag*

The Raman spectra are shown in Figures 8 and 9. In Raman spectra of slags, the vibration bands of the $[SiO_4]^{4-}$-tetrahedron can refer to the units of Q^n_{Si} (n = 0, 1, 2, 3…, number of bridging oxygen (BO) in silicates), which represent the degree of polymerization (DOP) of slags. As reported,[43,44] Q^0_{Si}, Q^1_{Si}, Q^2_{Si} and Q^3_{Si} are detected at the wavenumbers of ~ 860 cm^{-1} ($[SiO_4]^{4-}$, monomer), ~ 915 cm^{-1} ($[Si_2O_7]^{6-}$, dimer), ~ 980 cm^{-1} ($[Si_3O_{10}]^{8-}$, chain), and ~1060 cm^{-1} ($[Si_3O_9]^{6-}$, sheet), respectively. Similarly, the units of Q^2_{Al}, Q^3_{Al} and Q^4_{Al} in the stretching vibration of $[AlO_4]^{5-}$-tetrahedron correspond to the wavenumbers at ~740, ~790, and ~850 cm^{-1}, respectively.[36,45,46] On the other hand, according to previous studies,[47–50] the

Table II. Structural Units and Corresponding Raman Bands

Raman Shift (cm^{-1})	Assignments	References
400 to 700	T-O-T	[45, 46]
500 to 600	Al-O-Al	[45, 46]
~740	Q^2_{Al}	[36, 45, 46]
~790	Q^3_{Al}	[36, 45, 46]
~790	Ti-O stretching vibrations in $[TiO_4]^{4-}$	[19, 24, 25, 44, 50]
~850	Q^4_{Al}	[36, 41, 42]
~850	Ti-O stretching vibrations in $[Ti_2O_6]^{4-}$	[24, 25, 44, 50]
850 to 880	Q^0_{Si}	[44]
900 to 930	Q^1_{Si}	[44]
950 to 980	Q^2_{Si}	[44]
1040 to 1060	Q^3_{Si}	[44]

Raman band of $[TiO_6]^{8-}$ is at the wavenumbers of 600 to 650 cm^{-1}. As shown in Figure 8, there are no obvious peaks at 600 to 650 cm^{-1}, therefore the bands at ~790 and ~850 cm^{-1} reflect the stretching vibrations of Ti-O bond in $[TiO_4]^{4-}$ (monomer) and $[Ti_2O_6]^{4-}$ (chain), respectively.[24,25,44,50] In addition, the T-O-T (T: Al or Si) linkages are at the wavenumbers of 400 to 700 cm^{-1}.[45,46] Typically, the Al-O-Al bond mainly exists in the wavenumber range of 500 to 600 cm^{-1}.[46] Table II summarizes the structural units and their corresponding Raman bands.

The fractions of the structure units can be calculated semi-quantitatively according to the integrated area of the deconvoluted peaks. As shown in Table II, it is noted that both Q^3_{Al} and $[TiO_4]^{4-}$ correspond to the wavenumber at around 790 cm^{-1}, and similarly the wavenumber at around 850 cm^{-1} can be assigned to both Q^4_{Al} and $[Ti_2O_6]^{4-}$. Therefore, it is difficult to distinguish $Q^3_{Al}\backslash[TiO_4]^{4-}$ and $Q^4_{Al}\backslash[Ti_2O_6]^{4-}$ at the certain wavenumbers. Considering this aspect, the peaks at around 790 cm^{-1} and 850 cm^{-1} in this study are seen as the combined effects of $Q^3_{Al}+[TiO_4]^{4-}$ and $Q^4_{Al}+[Ti_2O_6]^{4-}$, respectively.

Figure 10 shows the deconvolution of the Raman spectra of the slags with different TiO_2 contents, and the relative fractions of Q^n_{Al} and Q^n_{Si} units in the slags are given in Figure 11. As shown in Figure 10(a), the units of Q^2_{Al}, Q^3_{Al} and Q^4_{Al} in the $[AlO_4]^{5-}$-tetrahedron and the units of Q^0_{Si}, Q^1_{Si} and Q^2_{Si} in the $[SiO_4]^{4-}$-tetrahedron are found, while Q^3_{Si} (1060 to 1200 cm^{-1}) could not be observed in the TiO_2-free slag system due to its low intensity. It is seen from Figure 11(a) that with the addition of TiO_2 into the slags, the fractions of $Q^4_{Al}+[Ti_2O_6]^{4-}$ and T-O-T bond decrease first and then increase; while the fractions of Q^2_{Al} and $Q^3_{Al}+[TiO_4]^{4-}$ show an opposite changing tendency. As shown in Table II, because Al-O-Al bond is at the wavenumber of 500 to 600 cm^{-1}, and the SiO_2 contents in the slags are very low (<9.5 pct, see Table I), the T-O-T in Figure 10 and Figure 11(a) are very likely Al-O-Al. In the case of silicate structure shown in Figure 11(b), an obvious

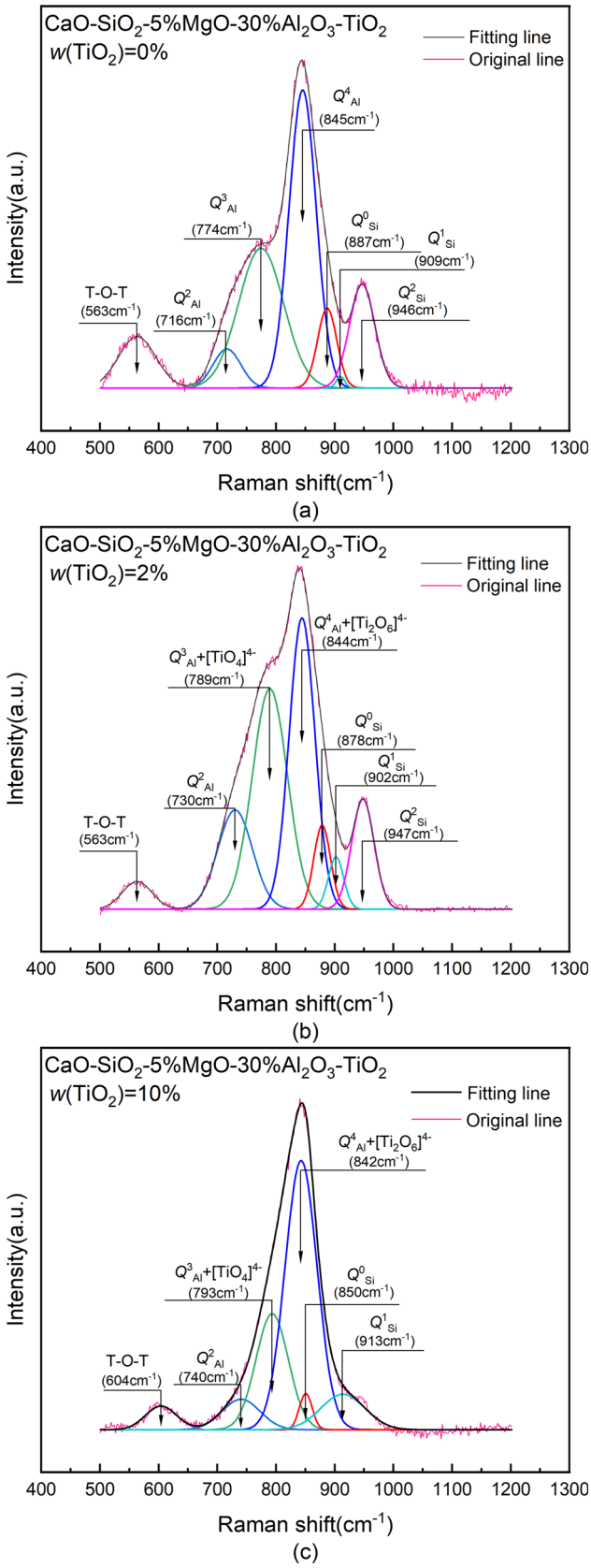

Fig. 10—Raman spectra of slags with different TiO_2 contents (R = 6). (*a*) $w(TiO_2)$ = 0 pct; (*b*) $w(TiO_2)$ = 2 pct; (*c*) $w(TiO_2)$ = 10 pct.

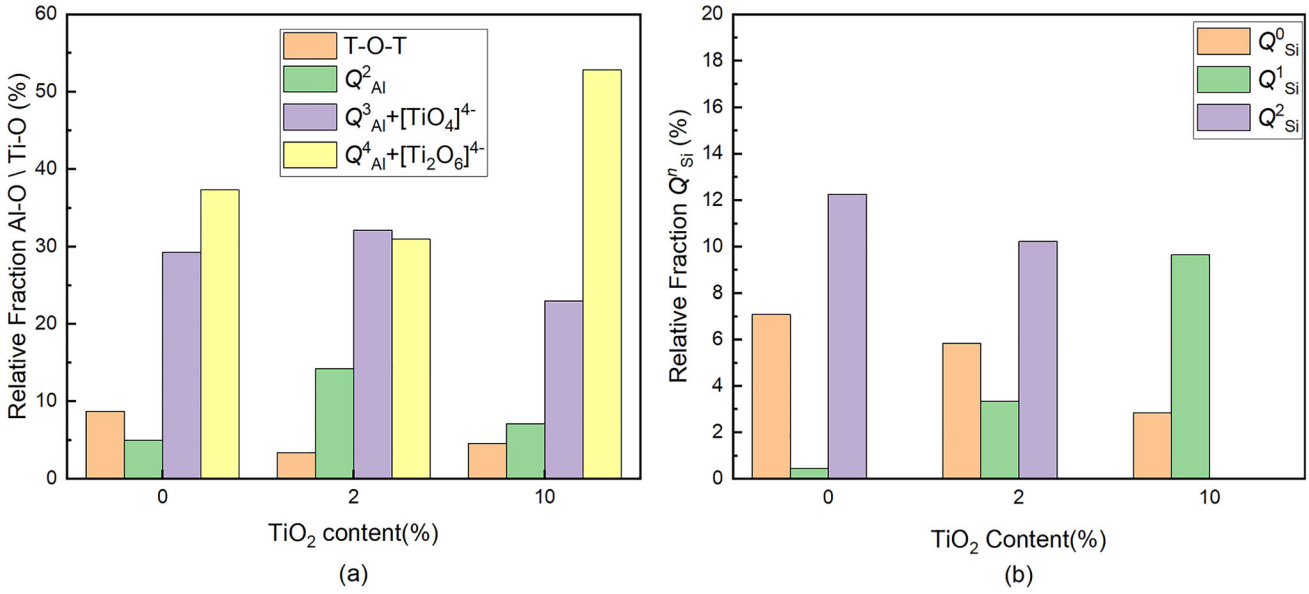

Fig. 11—Fractions of Al-O\Ti-O (*a*) and Q^n_{Si} (*b*) units in slags with different TiO_2 contents ($R = 6$).

increasing trend can be found in Q^1_{Si} with the increase of TiO_2 content in the slags. Besides, the fraction of Q^2_{Si} continues to decrease to almost zero, when the content of TiO_2 is 10 pct.

Figure 12 gives the deconvolution results of the Raman spectra of the slags with different basicity. The relative fractions of Al-O\Ti-O and Q^n_{Si} units in the slags are given in Figure 13 as well. It is seen from Figure 13(a) that T-O-T bond occupies the largest fraction when $R = 2$. When the basicity increases from 2 to 6, the T-O-T bond decreases, and the fractions of Q^2_{Al}, $Q^3_{Al}+[TiO_4]^{4-}$ and $Q^4_{Al}+[Ti_2O_6]^{4-}$ increase. When the basicity is further increased to 10, the T-O-T bond becomes not obvious, and a declining trend is found in the fractions of $Q^3_{Al}+[TiO_4]^{4-}$ and $Q^4_{Al}+[Ti_2O_6]^{4-}$. It is noted that the T-O-T bond in Figures 12 and 13(a) is probably Al-O-Al bond as well, because Al-O-Al band can decrease in frequency with the drop of SiO_2 content.[46] On the other hand, the proportion of silicate structure is getting lower and lower. As shown in Figure 13(b), the fractions of Q^1_{Si} and Q^2_{Si} continuously drop with increasing basicity, and Q^0_{Si} decreases first and then increases.

IV. DISCUSSION

A. *Activation Energy for Viscous Flow*

For a viscous flow, activation energy refers to the viscous flow barrier. According to the study of Litovitz *et al.*,[51] when the network structure of a viscous flow depolymerizes at high temperatures, the increased thermal motion is the reason to cause the change of activation energy. A higher temperature leads to a smaller activation energy. The relationship between temperature and slag viscosity can be described by Arrhenius equation, see Eq. [1].

$$\eta = \eta_0 \exp\left(\frac{E_\eta}{RT}\right) \quad [1]$$

where η, η_0, R, and T are viscosity, pre-exponent constant, activation energy, and the ideal gas constant as well as absolute temperature, respectively. Eq. [1] can be logarithmically written into Eq. [2].

$$\ln \eta = \ln \eta_0 + \frac{E_\eta}{R} \cdot \frac{1}{T} \quad [2]$$

Based on Eq. [2], Figure 14 plots the values of $\ln\eta$ against $1/T$. The apparent activation energies (E_η) therefore can be calculated from the slopes of the fitting lines of the plotted data. Table III lists the calculated activation energies of different slags. As shown in Table III, the activation energy decreases from 145.96 to 133.55 kJ/mol when the additional amount of TiO_2 rises from 0 to 2 pct; while it increases to 190.61 kJ/mol when the TiO_2 content further climbs to 10 pct in the slags ($R = 6$). It implies that the addition of TiO_2 influences the activation energy of the ladle slag system. Suitable addition amount of TiO_2 (*e.g.*, 2 pct) is favorable to lower the activation energy, leading to lower viscosity of the slags. On the other hand, with the increase of slag basicity from 2 to 10, the activation energy of the slags ($w(TiO_2) = 5$ pct) drops from 231.14 to 142.88 kJ/mol. The variation of activation energy is also in accordance with the change of slag viscosity.

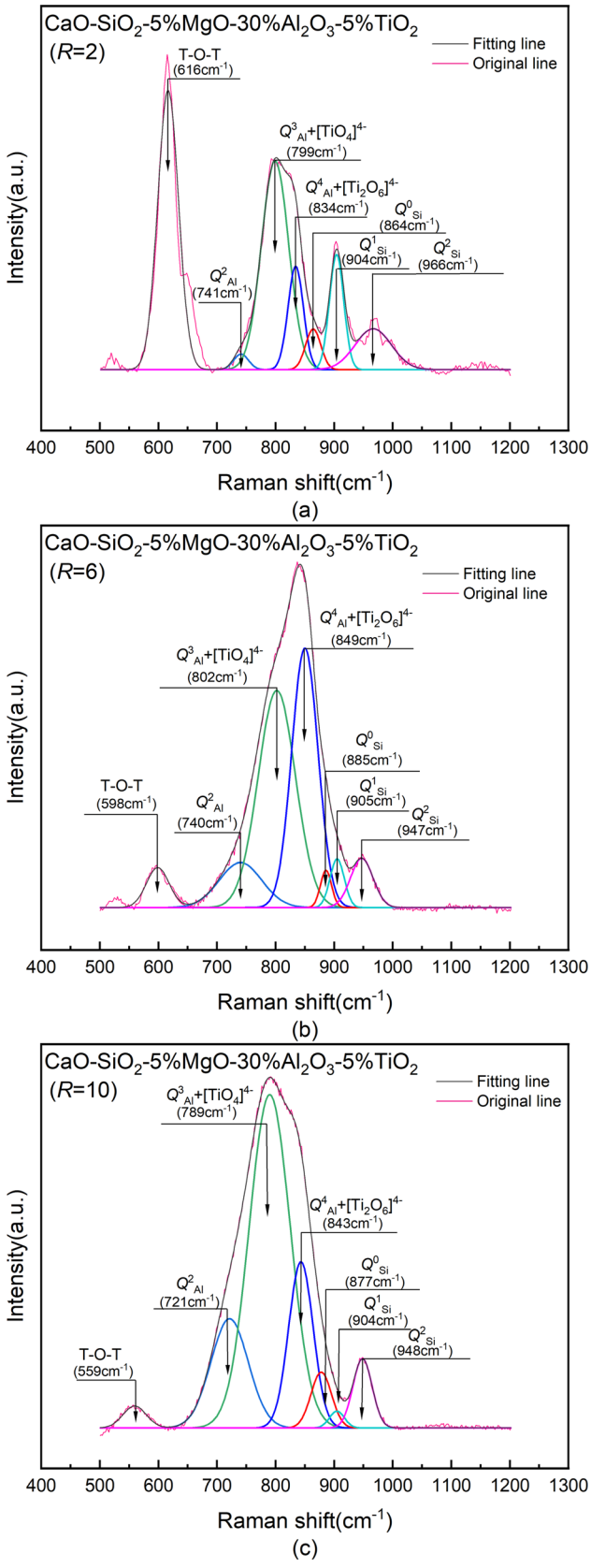

Fig. 12—Raman spectra of slags with different basicity ($w(TiO_2)$ = 5 pct). (*a*) R = 2; (*b*) R = 6; (*c*) R = 10.

B. *Effect of TiO_2 on Slag Structure*

Both Si and Al ions can be surrounded by four oxygen atoms to form a stable tetrahedron, namely $[AlO_4]^{5-}$ and $[SiO_4]^{4-}$. In charge balanced aluminosilicates, most $[SiO_4]^{4-}$ and $[AlO_4]^{5-}$ tetrahedron are polymerized to form bridging oxygen sites (BO), *e.g.*, Si-O-Si, Si-O-Al and Al-O-Al, with small amounts of non-bridging oxygens (NBO).[52] In the Raman spectra shown in Figures 10 and 12, T-O-T bond is presented. As reported in literature,[55–57] Al_2O_3 mainly presents in the form of $[AlO_4]^{5-}$ in high CaO and low SiO_2 slags. Generally, the ordering of framework in aluminosilicates is often described in terms of the Al avoidance rule, which states that two $[AlO_4]^{5-}$-tetrahedrons would never be linked.[53] Nevertheless, some researchers[54] pointed out that this rule is not applicable in amorphous aluminosilicates. Therefore, Al-O-Al is reasonable in this study.

As mentioned above, Al-O-Al bond is very likely to present the T-O-T structure in Figures 10 and 11(a). According to Figure 10(a), the Al-O band in Slag A1 should be Al-O-Al bond, Q^2_{Al}, Q^3_{Al} and Q^4_{Al} units, since no TiO_2 is contained in this slag. When 2 pct of TiO_2 is added in Slag A2, the fraction of Al-O-Al bond and $Q^4_{Al}+[Ti_2O_6]^{4-}$ unit decrease, while Q^2_{Al} and $Q^3_{Al}+[TiO_4]^{4-}$ units increase as shown in Figure 11(a). Because of the drop of Al-O-Al bond, the amount of bridge oxygens (BOs, O^0) in the slags decreases, and the aluminate is partially depolymerized. In this case, some of Q^4_{Al} is modified into Q^2_{Al} and Q^3_{Al}, resulting in the increase of Q^2_{Al} and Q^3_{Al}. On the other hand, due to the addition of TiO_2, the Ti-O bond should increase in Slag A2. Because $Q^4_{Al}+[Ti_2O_6]^{4-}$ unit decreases, the Ti-O bond should be mainly in the form of $[TiO_4]^{4-}$, not $[Ti_2O_6]^{4-}$. $[TiO_4]^{4-}$ monomer would weaken the slag structure as reported in Reference 58.

With further increase of TiO_2 content in the slags, the Al-O-Al bond and the structure of $Q^4_{Al}+[Ti_2O_6]^{4-}$ units increase, while Q^2_{Al} and $Q^3_{Al}+[TiO_4]^{4-}$ units decrease in Slag A5 ($w(TiO_2)$ = 10 pct) as shown in Figure 11(a). The FTIR spectra shown in Figure 6 also proves the climb of T-O-T band. The rise of Al-O-Al bond indicates the increase of BOs in the slag. However, the fraction of Al-O-Al bond in Slag A5 is still lower than that of Slag A1, therefore the fraction of Q^4_{Al} should be lower as well. On the other hand, the $[AlO_4]^{5-}$-tetrahedron structure is significantly increased compared with that in Slag A1. Because $Q^3_{Al}+[TiO_4]^{4-}$ unit decreases, it can be estimated that the Ti-O bond should be mainly in the form of $[Ti_2O_6]^{4-}$ unit. In this case, the evident increase of $Q^4_{Al}+[Ti_2O_6]^{4-}$ should be mainly due to the formation of $[Ti_2O_6]^{4-}$.

When an Al ion forms an $[AlO_4]^{5-}$-tetrahedron with the external oxygen atoms, charge compensation from cations is required.[59,60] In this study, due to the higher content of Al_2O_3 in the slags, $[AlO_4]^{5-}$-tetrahedron structure requires more charge compensation, in

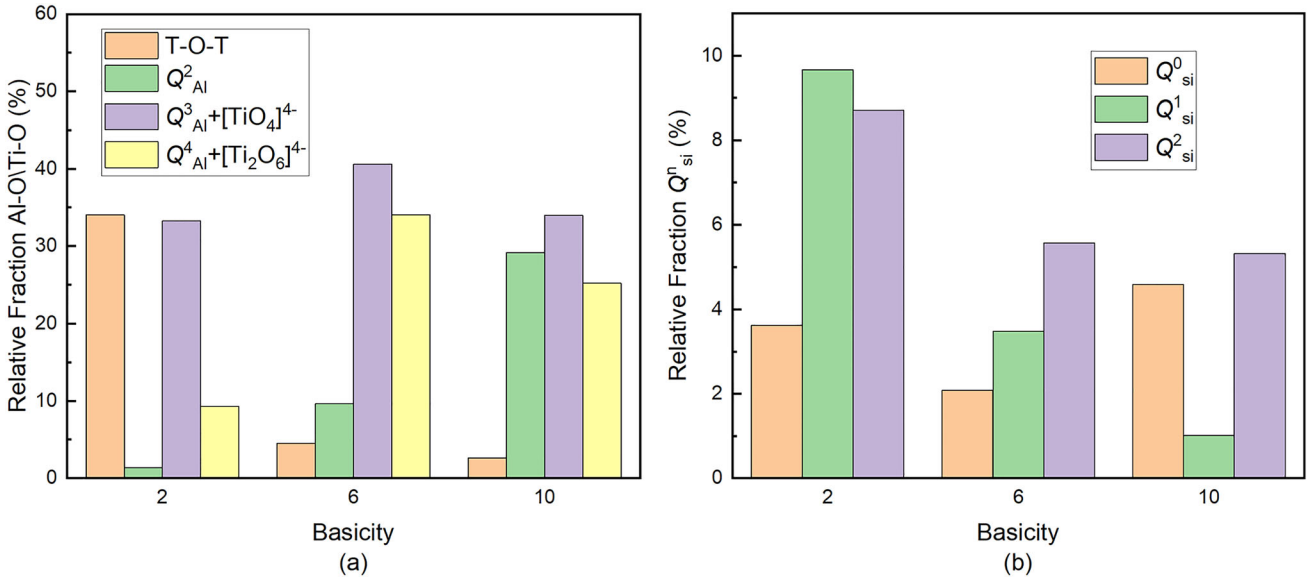

Fig. 13—Fractions of Al-O\Ti-O (*a*) and Q^n_{Si} (*b*) units in slags with different basicity ($w(TiO_2)$ = 5 pct).

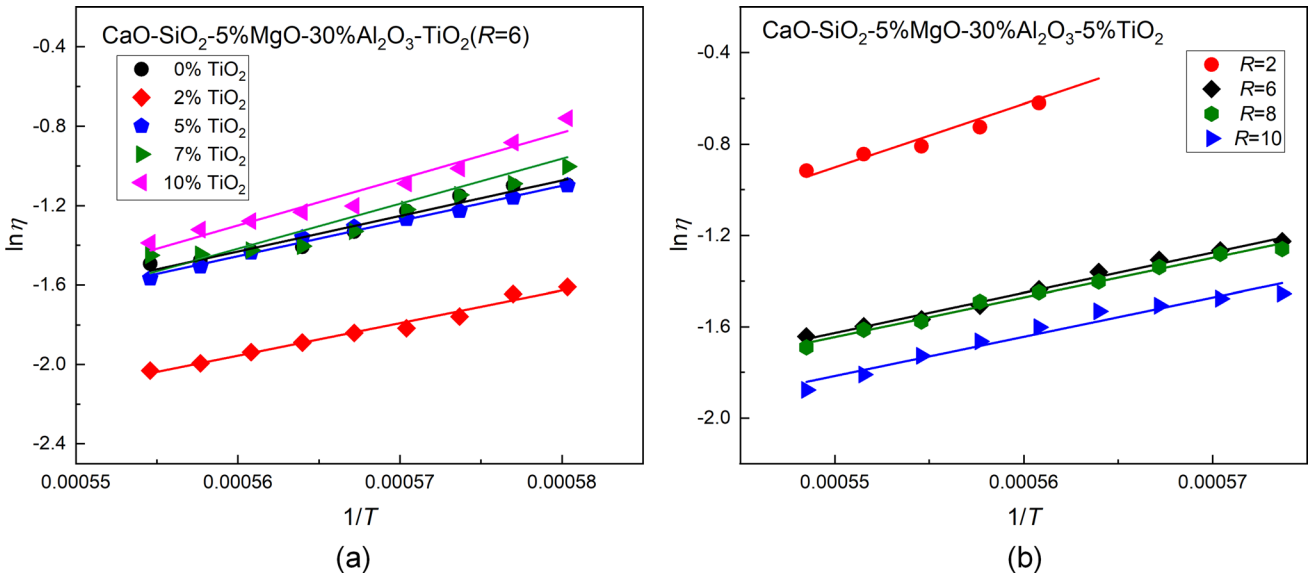

Fig. 14—Arrhenius plots of slags with different TiO_2 contents (*a*) and basicity (*b*).

Table III. Activation Energy of Slags

Slag No.	*R*	TiO_2 (Mass Pct)	E_η (kJ/mol)
A1	6	—	145.96
A2	6	2.00	133.55
A3	6	5.00	146.28
A4	6	7.00	184.80
A5	6	10.00	190.61
B1	2	5.00	231.14
B2	8	5.00	144.14
B3	10	5.00	142.88

contrast to $[SiO_4]^{4-}$-tetrahedron structure. As reported by Zheng *et al.*[24] $[Ti_2O_6]^{4-}$ unit can compete with silicate to coordinate Ca^{2+} so as to maintain the local charge balance in $CaO-SiO_2-TiO_2$ BF slag system. Consequently, a few NBOs linked to Si^{4+} turn into BOs, increasing the DOP of silicate network. Similarly, it can be inferred that $[Ti_2O_6]^{4-}$ can also compete with aluminate to coordinate Ca^{2+} and Mg^{2+}, making aluminate structure polymerize.

It can be seen that when a small amount of TiO_2 is added (*e.g.*, 2 pct, Slag A2) in the ladle slags, the Ti-O bond is mainly presented in the form of $[TiO_4]^{4-}$; it changes to $[Ti_2O_6]^{4-}$ as majority when the TiO_2 content is sufficiently high (*e.g.*, 10 pct, Slag A5). As mentioned above, the structure of $[TiO_4]^{4-}$ is monomer, while $[Ti_2O_6]^{4-}$ is in structure of chain. Therefore, different TiO_2 contents play different roles in $[AlO_4]^{5-}$-tetrahedron.

In terms of silicate structure, it is seen from Figure 11(b) that Q^1_{Si} unit increases, Q^0_{Si} and Q^2_{Si} units decrease with the addition of TiO_2 in the slags. It implies $[SiO_4]^{4-}$ tetrahedron is further depolymerized by TiO_2. Mysen *et al.*[60] proposed the depolymerization mechanism of silicate structure as shown in Eq. [3].

$$Q^0_{Si} + Q^2_{Si} = 2Q^1_{Si} \quad [3]$$

The free oxygen ions (O^{2-}) can react with BOs (O^0) in the viscous units of the network structures to form NBOs (O^-),[61] which can simplify the structure of the slag. Eq. [4] shows the reaction.

$$O^{2-} + O^0 = 2O^- \quad [4]$$

According to previous studies,[62] when Ti^{3+} ions are largely existed in the slags, the color of the quenched slags is purple. In this study, no purple slags were obtained. Therefore, titanium ions are very likely in the form of Ti^{4+}. Because TiO_2 can release O^{2-}, it can break the external silicate structure make it be depolymerized. This is consistent with previous studies.[12–14,16,19–23] In these studies, BF slag system was considered. The viscosity of the slags decreased with the addition of TiO_2.

Although TiO_2 can modify the structure of silicates as reported in literature,[13–17] it has different impact on the structure of aluminate depending on its content as mentioned above. In this study, the ladle refining slags contain a low SiO_2 content and a high Al_2O_3 content. So, more $[AlO_4]^{5-}$-tetrahedrons should be existed in the slags, and the structure variation of $[AlO_4]^{5-}$-tetrahedron (Q^2_{Al}, Q^3_{Al} and Q^4_{Al}) should play more profound role in the change of viscosity. A low TiO_2 content in the ladle slags can weaken the strength of the slag structure according to the formation of $[TiO_4]^{4-}$, while sufficient TiO_2 will lead to the formation of $[Ti_2O_6]^{4-}$, and further increase the DOP of the slags. Meanwhile, the changing trend of viscosity is also in line with the calculated activation energies, see Table III. As a result, the slag viscosity decreases first and then increases with the addition of TiO_2 in the slags.

C. *Effect of Basicity on Slag Structure*

As shown in Figures 7 and 13(a), with the increase of slag basicity, T-O-T bond declines, and Q^2_{Al} increases. Besides, the fraction of $Q^3_{Al} + [TiO_4]^{4-}$ and $Q^4_{Al} + [Ti_2O_6]^{4-}$ units first increases and then decreases. Meanwhile, it can also be seen from Figure13(b) that, the fraction sum of Q^n_{Si} units drops with slag basicity, and the ratio of simple unit Q^0_{Si} climbs in the Q^n_{Si} units. These results indicate that both the aluminate and silicate structures are impacted by slag basicity.

There are many publications[4,20,25,36] indicate that CaO as a basic oxide can change the slag structure by providing free oxygen ions (O^{2-}). O^{2-} can combine with Si and Al cations in $[AlO_4]^{5-}$ and $[SiO_4]^{4-}$ structures to break BOs, and depolymerize the complex structures into simpler ones. It is seen from Figure 13(a) that when $R = 2$, T-O-T bond dominates the structure. With the increase of slag basicity (*e.g.*, $R = 6$), some of the T-O-T bond is broken by the free oxygen ions. On the other hand, due to the decrease of SiO_2 content in the slags, the proportion of silicate structure becomes smaller, making aluminates structure more profound. When the basicity further increases to 10, although T-O-T bond is further depolymerized, the change is relatively small, and some of $Q^4_{Al} + [Ti_2O_6]^{4-}$ and $Q^3_{Al} + [TiO_4]^{4-}$ units are modified into Q^2_{Al} unit, leading to the increase of NBOs. McMillan *et al.*[45] also reported that adding CaO to aluminates would result in an unstable network of depolymerized aluminate tetrahedron groups. Additionally, due to the rise of free oxygen ions in the slags, the silicate structure is also modified into simpler units, see Figure 13(b). This is in line with the results in literature.[20,25]

It is noted that the Al_2O_3 contents (30 pct) in the experimental slags are much higher than that of SiO_2, even the slag basicity is 2. As discussed above, the structure of $[AlO_4]^{5-}$-tetrahedron may play more profound role in the viscosity due to the low content of SiO_2 in the slags in this study. Considering the wavenumbers of the T-O-T structure shown in Figures 9 and 12, it can be estimated that Al-O-Al bond is more likely in contrast to Si-O-Si bond (at 600 to 750 cm^{-1}[63]), even when $R = 2$. In the study of Kim and Park,[36] Al-O-Al was also taken into account in $CaO\text{-}SiO_2\text{-}Al_2O_3\text{-}MgO\text{-}CaF_2$ slag system with 24 to 35 pct of Al_2O_3. On the other hand, the consideration of T-O-T in this study seems more comprehensive, because it can avoid incorrect assignments, and doesn't influence the discussion on the effects of TiO_2 and basicity as well.

Additionally, as shown in Table III, with the increase of basicity, the calculated activation energy decreases as well. Therefore, the slag viscosity should decline with the rise of slag basicity. In the present study, even though some TiO_2 is added in the slags, the effect of basicity on the viscosity of the slags presents the same trend.

As mentioned above, a small amount of TiO_2 can improve the fluidity of the ladle refining slags. In a previous study of the present authors,[39] it was also found that a small amount of TiO_2 can lower the melting point of the ladle slags. Therefore, the addition of TiO_2 into ladle refining slags is possible for the refining of Ti-bearing steel grades. Even though, future studies are still needed to understand the effect of TiO_2-containing slags on steel cleanliness.

V. CONCLUSIONS

In this study, the effect of TiO_2 on the viscosity of a TiO_2-containing ladle refining slag system was investigated. The main conclusions are listed as follows.

1. With the increase of TiO_2 content in the slag system, the viscosity of the slags decreases first and then increases. A low TiO_2 content (*e.g.*, 2 pct) in the ladle slags can weaken the strength of the slag structure according to the formation of $[TiO_4]^{4-}$; while sufficient TiO_2 (*e.g.*, 10 pct) will lead to the formation of $[Ti_2O_6]^{4-}$, and further increase the DOP of the slags.

Although silicate structure can be depolymerized by TiO_2, the aluminate structure variation plays more profound role in the change of viscosity in the study.
2. With the increase of slag basicity, the viscosity of the slag system decreases. The free oxygen provided by CaO decreases the DOP of both aluminate and silicate structures in the TiO_2 containing slags.
3. Due to the positive effect on melting point and viscosity, the addition of TiO_2 into ladle refining slags is very possible for the refining of Ti-bearing steel grades.

ACKNOWLEDGMENT

This study was funded by the National Natural Science Foundation of China (U20A20272 and 52074073) and the Fundamental Research Funds for the Central Universities (N2325035).

CONFLICT OF INTEREST

On behalf of all authors, the corresponding author states that there is no conflict of interest.

REFERENCES

1. Y. Gordon, S. Kumar, M. Freislich, and Y. Yaroshenko: *Steel Transl.*, 2015, vol. 45, pp. 627–34.
2. M. Iwasaki and M. Matsuo: *Nippon Steel Technical Report*, 2011, vol. 391, pp. 88–93.
3. T. Zervas, J.T. McMullan, and B.C. Williams: *Int. J. Energy Res.*, 1996, vol. 20, pp. 69–91.
4. J.J. Pak, J.O. Jo, S.I. Kim, W.Y. Kim, T.I. Chung, S.M. Seo, J.H. Park, and D.S. Kim: *ISIJ Int.*, 2007, vol. 47, pp. 16–24.
5. L. Zhang, L.N. Zhang, M.Y. Wang, G.Q. Li, and Z.T. Sui: *Miner. Eng.*, 2007, vol. 20, pp. 684–93.
6. X. Xing, Z. Pang, and C. Mo: *J. Non-Cryst. Solids*, 2020, vol. 530, 119801.
7. Z.J. Wang, Q.F. Shu, S. Sridhar, M. Zhang, M. Guo, and Z.T. Zhang: *Metall. Mater. Trans. B*, 2015, vol. 46B, pp. 758–65.
8. G.R. Li: *J. Iron. Steel Res. Int.*, 2003, vol. 10, pp. 6–9.
9. Z.L. Piao, L.G. Zhu, X.J. Wang, B. Wang, P.C. Xiao, and Z.P. Yuan: *Metall. Mater. Trans. B*, 2020, vol. 51, pp. 2119–30.
10. H.L. Fan, R.X. Wang, Z.F. Xu, H.M. Duan, and D.F. Chen: *J. Non-Cryst. Solids*, 2021, vol. 571, 121049.
11. J.L. Li, Q.F. Shu, and K.C. Chou: *Can. Metall. Q.*, 2015, vol. 54, pp. 85–91.
12. Z.Y. Chang, K.X. Jiao, J.L. Zhang, X.J. Ning, and Z.Q. Liu: *ISIJ Int.*, 2018, vol. 58, pp. 2173–79.
13. Y.H. Gao, L.T. Bian, and Z.Y. Liang: *Steel Res. Int.*, 2015, vol. 86, pp. 386–90.
14. J.L. Fang, Z.G. Pang, X.D. Xing, and R.S. Xu: *Materials*, 2020, vol. 14, p. 124.
15. W.J. Huang, Y.H. Zhao, S. Yu, L.X. Zhang, Z.C. Ye, N. Wang, and M. Chen: *ISIJ Int.*, 2016, vol. 56, pp. 594–601.
16. D. Yang, H.H. Zhou, J. Wang, Z.D. Pang, G.S. Pei, Z.M. Yan, H.X. Mao, G.B. Qiu, and X.W. Lv: *J. Mater. Res. Technol.*, 2021, vol. 12, pp. 1615–22.
17. C. Feng, L.H. Gao, J. Tang, Z.G. Liu, and M.S. Chu: *Trans. Nonferrous Met. Soc. China*, 2020, vol. 30, pp. 800–11.
18. J.F. Li, Z.L. Xu, H. Yang, L.Y. Yu, and M. Liu: *Appl. Surf. Sci.*, 2009, vol. 255, pp. 4725–32.
19. Z.G. Pang, X.D. Xing, J.L. Zheng, Y.L. Du, S. Ren, and M. Lv: *J. Non-Cryst. Solids*, 2021, vol. 571, 121071.
20. H. Park, J.Y. Park, G.H. Kim, and I. Sohn: *Steel Res. Int.*, 2012, vol. 83, pp. 150–56.
21. I. Sohn, W.L. Wang, H.Y. Matsuura, F. Tsukihashi, and D.J. Min: *ISIJ Int.*, 2012, vol. 52, pp. 158–60.
22. A. Ohno and H.U. Ross: *Can. Metall. Q.*, 1963, vol. 2, pp. 259–79.
23. J.L. Liao, J. Li, X.D. Wang, and Z.T. Zhang: *Ironmak. Steelmak.*, 2012, vol. 39, pp. 133–39.
24. K. Zheng, Z.T. Zhang, L.L. Liu, and X.D. Wang: *Metall. Mater. Trans. B*, 2014, vol. 45B, pp. 1389–97.
25. S.F. Zhang, X. Zhang, L. Wei, X.W. Lv, C.G. Bai, and L. Wang: *J. Non-Cryst. Solids*, 2014, vol. 402, pp. 214–22.
26. Z.M. Yan, X.W. Lv, W. He, and J. Xu: *ISIJ Int.*, 2017, vol. 57, pp. 31–36.
27. X.J. Dong, H.Y. Sun, X.F. She, Q.G. Xue, and J.S. Wang: *Ironmak. Steelmak.*, 2014, vol. 41, pp. 99–106.
28. G.X. Qiu, D.J. Miao, M.C. Cai, X.M. Li, D.P. Zhan, and Y.F. Liu: *Iron Steel*, 2022, vol. 57, pp. 42–52.
29. J.Z. Zhang and L.L. Shi: *J. Iron Steel Res.*, 2010, vol. 22, pp. 16–19.
30. Z.D. Pang, X.W. Lv, Y.Y. Jiang, J.W. Ling, and Z.M. Yan: *Metall. Mater. Trans. B*, 2020, vol. 51B, pp. 722–31.
31. K. Hu, K. Tang, X.W. Lv, S. Jafar, Z.M. Yan, and B. Song: *Metall. Mater. Trans. B*, 2021, vol. 52B, pp. 245–54.
32. S.Q. Zhang, K. Zheng, J.X. Jiang, S.Y. Zhang, and G. Xu: *J. Mater. Res. Technol.*, 2021, vol. 15, pp. 2686–86.
33. J.Y. Xiang, J. Wang, Q.J. Li, C. Shan, G.B. Qiu, W.Z. Yu, and X.W. Lv: *Can. Metall. Q.*, 2020, vol. 59, pp. 151–58.
34. J.F. Li, J.G. Huang, H. Feng, X.Y. Wang, X.C. Yin, and Y.T. Zhang: *J. Non-Cryst. Solids*, 2022, vol. 576, 121243.
35. G. Handfield and G.G. Charette: *Can. Metall. Q.*, 1971, vol. 10, pp. 235–43.
36. T.S. Kim and J.H. Park: *ISIJ Int.*, 2014, vol. 54, pp. 2031–38.
37. S.C. Zhang, H.B. Li, M.Z. Ran, and Z.H. Jiang: *ISIJ Int.*, 2022, vol. 62, pp. 2207–16.
38. P.G. Jönsson, L. Jönsson, and D. Sichen: *ISIJ Int.*, 1997, vol. 37, pp. 484–91.
39. X.M. Zhang, Z.W. Yan, Z.Y. Deng, and M.Y. Zhu: *Metals*, 2023, vol. 13, p. 431.
40. M.K. Sun, I.H. Jung, and H.G. Lee: *Met. Mater. Int.*, 2008, vol. 14, pp. 791–98.
41. C. Feng, M.S. Chu, J. Tang, Y.T. Tang, and Z.G. Liu: *Steel Res. Int.*, 2016, vol. 87, pp. 1274–83.
42. S.M. Han, J.G. Park, and I. Sohn: *J. Non-Cryst. Solids*, 2011, vol. 357, pp. 2868–75.
43. X. Shen, M. Chen, N. Wang, and D. Wang: *ISIJ Int.*, 2019, vol. 59, pp. 9–15.
44. B.O. Mysen, F.J. Ryerson, and D. Virgo: *Am. Miner.*, 1980, vol. 65, pp. 1150–65.
45. P. McMillian and B. Piriou: *J. Non-Cryst. Solids*, 1983, vol. 55, pp. 221–42.
46. D.R. Neuville, L. Cormier, and D. Massiot: *Chem. Geol.*, 2006, vol. 229, pp. 173–85.
47. K. Zheng, J. Liao, X.D. Wang, and Z.T. Zhang: *J. Non-Cryst. Solids*, 2013, vol. 376, pp. 209–15.
48. F. Farges, G.E. Brown Jr., and J.J. Rehr: *Geochim. Cosmochim. Acta*, 1996, vol. 60, pp. 3023–38.
49. Z.M. Yan, X.W. Lv, and Z.S. Li: *J. Iron Steel Res.*, 2022, vol. 29, pp. 187–206.
50. S. Ren, Q. Zhao, L. Yao, and Q.C. Liu: *CrystEngComm*, 2016, vol. 18, pp. 1393–1402.
51. P.B. Macedo and T.A. Litovitz: *J. Chem. Phys.*, 1965, vol. 42, pp. 245–56.
52. J.F. Stebbins and Z. Xu: *Nature*, 1997, vol. 390, pp. 60–62.
53. W. Loewenstein: *Am. Mineral.*, 1954, vol. 39, pp. 92–96.
54. S.K. Lee and J.F. Stebbins: *J. Non-Cryst. Solids*, 2000, vol. 270, pp. 260–64.
55. G.S. Henderson: *Can. Mineral.*, 2005, vol. 43, pp. 1921–58.
56. P. McMillan: *Am. Miner.*, 1984, vol. 69, pp. 622–44.
57. G.H. Kim and I. Sohn: *ISIJ Int.*, 2012, vol. 52, pp. 68–73.
58. Z. Wang, Q. Shu, and K. Chou: *Steel Res. Int.*, 2013, vol. 84, pp. 766–76.

59. S. Xie, R. Li, T. Yuan, M. Zhang, M. Wang, H. Wu, and F. Zeng: *Scr. Mater.*, 2018, vol. 149, pp. 125–28.
60. B. Mysen and P. Richet: *Silicate Glasses and Melts*, 2nd ed. Elsevier, Candice Janco, 2018, pp. 230–40.
61. Y.M. Gao, S.B. Wang, C. Hong, X.J. Ma, and F. Yang: *Int. J. Miner. Metall. Mater.*, 2014, vol. 21, pp. 353–62.
62. T. Hashimoto, H. Nasu, and K. Kamiya: *J. Am. Ceram. Soc.*, 2006, vol. 89, pp. 2521–27.
63. J.X. Gao, G.H. Wen, T. Huang, B.W. Bai, P. Tang, and Q. Liu: *J. Non-Cryst. Solids*, 2016, vol. 452, pp. 119–24.